Superconducting high-pressure phase of platinum hydride from first principles

Xiang-Feng Zhou (周向锋), Artem R. Oganov, Xiao Dong (董晓), Lixin Zhang (张立新), Yongjun Tian (田永君), and Hui-Tian Wang (王慧田)

Superconducting high pressure phase of platinum hydride from first principles

Xiang-Feng Zhou (周向锋),[1,2] Artem R. Oganov,[3,4] Xiao Dong (董校),[1]
Lixin Zhang (张立新),[1] Yonjun Tian (田永君),[5] and Hui-Tian Wang (王慧田)[1,2,*]

[1]*School of Physics and Key Laboratory of Weak-Light Nonlinear Photonics, Nankai University, Tianjin 300071, China*
[2]*National Laboratory of Solid State Microstructures, Nanjing University, Nanjing 210093, China*
[3]*Department of Geosciences, Department of Physics and Astronomy,*
and New York Center for Computational Sciences, Stony Brook University, Stony Brook, New York 11794-2100, USA
[4]*Department of Geology, Moscow State University, 119992 Moscow, Russia*
[5]*State Key Laboratory of Metastable Materials Science and Technology, Yanshan University, Qinhuangdao 066004, China*

Recently a superconducting transition was found in silane in high-pressure experiments. However, the experimental x-ray diffraction (XRD) patterns do not match any one of proposed silane structures, and it has been suggested to be originated from a platinum hydride. Neither the structure nor superconductivity of any platinum hydride is known. Here the underlying physics behind the anomalous superconducting transition in experiment is revealed by first-principles calculations. We predict a stable hexagonal $P6_3/mmc$ phase of platinum hydride at high pressure. Its lattice constants and simulated XRD pattern are in excellent agreement with the experimental results. The superconducting transition temperatures in this phase are found to coincide with the measured values, too. This discovery provides new insights into the unusual superconducting behavior reported for silane.

I. INTRODUCTION

An exotic and appealing prediction going back to the early 1930's was that of metallic hydrogen, which is a potential high T_c superconductor at high pressures.[1,2] However, hydrogen remained an insulator even up to the pressure of 342 GPa.[3] Recently, it was suggested that hydrogen-rich group IV hydrides can be metalized at much lower pressures because of the "chemical precompression" caused by the group IV atoms.[4–11] Therefore, much theoretical and experimental effort has focused on the possibility of attaining high-temperature superconductivity in group IV hydrides. The particular interesting is the case of silane (SiH$_4$), which was predicted to have at least seven phases.[10,11] Only one solid phase has been reported in the pressure range between 10 and 25 GPa with a monoclinic structure at room temperature.[12] At pressure above 60 GPa, Chen *et al.*[13] found the pressure-induced metallization for silane by analyzing the infrared reflectivity data at room temperature.

The most recent experiments showed the transformation of an insulating silane to a metal at 50 GPa, becoming superconducting at a transition temperature T_c = 17.5 K at 96 GPa and 17 K at 120 GPa. If the sample is further compressed, it transforms into a transparent $I41/a$ phase. The metallic phases could coexist with the transparent one up to the highest experimental pressure of 192 GPa.[14] Most strikingly, it shows an abnormal non-monotonic dependence of T_c on pressure in the range from 65 to 192 GPa. However, the crystal structure of metallic silane is not fully resolved, still less for the origin of the superconductivity. The $P6_3$ structure of superconducting silane proposed in Ref. 14 is impossible from the theoretical viewpoint: it is dynamically unstable and does not produce the observed equation of state.[14] Such an unexpected difficulty in reconciling experimental and theoretical structures and unusual compression behavior raises at least two important questions: (i) what is the exact structure of this metallic phase above 100 GPa? (ii) what is the physical origin

behind the anomalous superconducting transition behavior in experiment? Many independent works have predicted the insulating $I41/a$ structure to be the most stable phase from 50 to 220 GPa,[6,10,11] while experiments presented a $P6_3$ structure.[14] Moreover, as alluded above, the $P6_3$ structure of silane is dynamically unstable in this pressure range and is energetically quite unfavorable.[10,11] Subsequently, *Cmca* and *Pbcn* phases have been predicted to be the most likely phases for the metallic silane,[10,11] but both do not match the experimental x-ray diffraction (XRD) pattern and are thermodynamically more favorable than the insulating $I41/a$ phase only above 220 GPa. Consequently, although many efforts have been made to elucidate the novel structures and properties, some features of metallic silane remained elusive.

Degtyareva *et al.*[15] showed that the experimental XRD pattern can be explained by the formation of a platinum hydride due to the reaction of hydrogen (originating from the decomposed silane) with platinum electrodes (used for measuring conductivity). However, the structure and exact composition of this platinum hydride are not determined, and it is still unknown whether platinum hydride(s) can explain peculiar superconductivity observed in Ref. 14. Here we will unveil these outstanding questions by using the first-principles calculations.

II. METHOD

Database searching and structure construction from different orientations of archetypal crystals manually are employed to do structure prediction.[16–18] Moreover, to make sure the reliability of our predicted structure, the additional *ab initio* evolutionary algorithm is carried out for structural identification.[19] We have performed the detailed evolutionary simulations for four fixed stoichiometries (PtH, PtH$_2$, Pt$_2$H, and Pt$_2$H$_3$) at 120 GPa (6 and 12 atoms per unit cell for PtH, PtH$_2$ and Pt$_2$H, and 10 atoms per unit cell for Pt$_2$H$_3$,

respectively). We have also done additional evolutionary simulation for PtH with 12 atoms per unit cell, and confirmed that $P6_3/mmc$ (NiAs-type) PtH is the most stable phase at 113 GPa and $Fm\bar{3}m$ (NaCl-type) PtH will be the most stable one at 120 GPa. Calculations are performed within the generalized gradient approximation (GGA) using the projector augmented wave method as implemented in the VASP code.[20] We employ the plane-wave cut-off energy of 500 eV and a Monkhorst-Pack Brillouin zone sampling grid with the resolution of $2\pi \times 0.25$ Å^{-1}. With the electronic self-consistency threshold of 10^{-5} eV/cell, relaxation proceeded until forces on atoms became smaller than 10^{-2} eV/Å. In addition, in the PtH$_x$ system the formation enthalpy, defined as $\Delta H = \{H(\text{PtH}_x) - [A \times H(\text{Pt}) + B \times H(\text{H})]\}/(A + B)$, is an important factor for evaluating the energetic stability, where $H(\text{PtH}_x)$ is the enthalpy of PtH$_x$ per unit cell. $H(\text{Pt})$ and $H(\text{H})$ are the enthalpy of fcc-Pt and monoclinic ($C2/c$) hydrogen (per atom) at a certain pressure, respectively. A and B are the numbers of Pt and H atoms per unit cell for PtH$_x$. To check dynamical stability, we compute phonon dispersion curves at various pressures using density functional perturbation theory (DFPT) as implemented in the QUANTUM ESPRESSO package.[21] These calculations use the same GGA-PW91 exchange-correlation functional,[22] Vanderbilt ultrasoft potentials with a cutoff energy of 50 Ry for the wave functions, $24 \times 24 \times 12$ Monkhorst-Pack k-point grids with Gaussian smearing of 0.05 Ry. Dynamical matrices are determined on a $6 \times 6 \times 3$ q-point mesh, and double k-point grids are used for the calculation of electron-phonon interaction matrix elements. We also test denser k-point and q-point sets, but find no substantial differences in results. Powder XRD patterns are simulated using the REFLEX software.[23]

III. RESULTS AND DISCUSSION

As listed in Table I, the calculated lattice constants of $I4_1/a$ silane are in good agreement with the experimental values at 160 GPa,[14] implying that the VASP-GGA method is valid for this simulation. Our structure searching has revealed many possible candidates, among them the most interesting two are Ni$_2$H-type Pt$_2$H ($P\bar{3}m1$ symmetry) and NiAs-type PtH ($P6_3/mmc$ symmetry), because their calculated lattice constants match the experimental values at 113 and 160 GPa (see Table I).[14] We also should note that the theoretical pressures are systematically shifted with respect to experimental one by 10-15 GPa, but this has a very minor effect on the lattice constants or electron-phonon coupling (EPC) calculation above in this case. Figures 1(a) and (b) show the structure of the newly predicted hexagonal metal-sandwich $P6_3/mmc$ PtH phase, in which the Pt atoms occupy the 2c (0.333, 0.667, 0.25) sites and the H atoms occupy the 2a (0.0, 0.0, 0.0) sites. Most importantly, the calculated relative enthalpy diagram of PtH$_x$ in Fig. 1(c) suggests that the $P6_3/mmc$ PtH phase is the most stable one at 113 GPa,[19] indicating that it should be a more suitable candidate than $P\bar{3}m1$ Pt$_2$H.

To further confirm the above mentioned opinion, we simulate the XRD patterns of PtH and Pt$_2$H, compared with the experimental XRD pattern at 113 GPa, as shown in Fig. 2(a). The peak position and intensity of PtH are in good agreement with the experimental data.[14] However, the peak position of Pt$_2$H has a tiny shift with respect to the experimental data. It should be pointed out that the discrepancy for the experimentally observed 111 peak is from the gasket of cubic BN. For the theoretically predicted 202 and 104 peaks, both are not very clear but are still dimly visible in the experimental XRD pattern. When considering the possibility of the existence of an unknown metallic silane phase during this stage, distinguishing the exact peaks is very difficult because almost all of the peaks of the unknown metallic silane could be hidden among the reflections of PtH. As shown in Fig. 2(b), a similar trend is observed at 160 GPa, in both cases for convenience, we keep a constant weight (90% of silane and 10% of PtH) for the simulation. As there is a great overlap for peaks among these phases, at the 121, 015, and 024 peaks, a mixture of these phases could explain the experimental peaks.

The dynamical stability of the $P6_3/mmc$ PtH phase has been examined through phonon calculations at 113 GPa. As shown in Fig. 3(a), the absence of imaginary frequency modes indicates this structure to be stable. Additional phonon calculations at 90, 100, 130, 160, and 192 GPa (are not shown here) indicate that PtH is also dynamically stable within the pressure range from 113 to 192 GPa, but develops soft modes below 100 GPa.[19] This is consistent with the experimental observations and can explain why the integrity of the sample is preserved only when the sample is warmed to 300 K under the pressure above 100 GPa.[14] Figure 3(b) shows the band structure of PtH at 113 GPa. It reveals metallic character with large dispersion bands crossing the Fermi level (E_F) and a relatively flat band in the vicinity of E_F close to the L point [see the line with solid squares in Fig. 3(b)]. The coexistence of flat and steep bands near the Fermi level has been suggested as a favorable condition for enhancing Cooper pair formation, which is essential to superconducting behavior.[7] Therefore, we perform the EPC calculations to explore the possible superconductivity, as shown in Fig. 4(a). The calculated Eliashberg phonon spectral function $\alpha^2F(\omega)$, logarithmic average phonon frequency ω_{log}, and the EPC strength λ at different pressures are listed in Table II. The superconducting temperature T_c could be estimated from the Allen-Dynes modified McMillan equation, by using $T_c = (\omega_{log}/1.2) \exp\{-[1.04(1 + \lambda)]/[\lambda - \mu^*(1 + 0.62\lambda)]\}$.[24] For estimating T_c, the following parameters are used: a typical value of Coulomb pseudopotential $\mu^* = 0.1$ (for most materials, μ^* takes values between $0.10 - 0.14$ and the associated uncertainty on T_c is usually $\sim 15 - 20\%$),[7,10,25,26] a calculated $\lambda = 0.85$ at 113 GPa (which indicates the strong EPC), and a calculated $\omega_{log} = 328.66$ K. Thus, we predict $T_c = 17.2$ K, which is in good agreement with experimental result $T_c = 17$ K.[14] At 113 GPa, the heavy Pt atoms dominate the low-frequency vibrations, while the light H atoms contribute significantly to the high-frequency modes [see the dotted line in Fig. 4(b)]. The low-frequency Pt vibrations and the high-frequency H vibrations in the PtH phase at 113 GPa contribute 52% and 48% to the EPC strength λ, respectively. Therefore, it is suggested that the Pt atoms play a significant

role in the superconductivity of PtH at 113 GPa. As the pressure increases, these contributions are changed to be 31% and 69% at 130 GPa, 34% and 66% at 160 GPa, 35% and 65% at 192 GPa, respectively. It implies that the contribution to the high T_c from the H atoms will exceed that of the Pt atoms when the pressure is above 160 GPa, and stays almost constant up to 192 GPa. In contrast, the EPC calculations show that $P\bar{3}m1$ Pt_2H has the superconducting transition temperature of ~1 K, which is much lower than the experimental value of 17 K at 113 GPa.[14] Thus, it should be excluded for the present discussion.

Our present results show that T_c of PtH decreases monotonically as the pressure increases from 113 to 192 GPa, which agrees with the experimental data from 100 to 160 GPa very well,[14] but cannot explain the abnormal transition at 192 GPa. There is one possibility: just as Chen *et al.*[10] pointed out that the metallic silane may have the fluctuating transition temperature as the pressure increases. However, the *Cmca* silane is still not confirmed by experiment. In theory, there is a better candidate *Pbcn* silane structure, which seems to be the most stable structure above 220 GPa, but the only available T_c data point is at 190 GPa (the estimated value of T_c = 16.5 K and the measured value of 12 K).[11] Therefore, we propose other possible interpretation that PtH dominates the superconducting transition temperature within the pressure range from 113 to 160 GPa. When the pressure is above 192 GPa, the metallic *Pbcn* silane may form and be responsible for the high T_c.[11] In such a way, it will be consistent with other independent experimental observation (even there is still ambiguity) that there is an insulator-semiconductor phase transition between 92 and 109 GPa, while a much higher pressure (above 210 GPa) is needed for the metallization in silane.[27]

IV.   CONCLUSION

In summary, by performing the first-principle calculations, we predict a new high-pressure phase of platinum hydride, $P63/mmc$ PtH, which may exist experimentally but has never been confirmed so far.[15] This discovery gives a well explanation for the differences between experimental and theoretical studies of high pressure phase of silane.[6,8,10,11,14] The calculated lattice constants, the simulated XRD pattern, and the superconducting transition temperature for platinum hydride are in good agreement with the previously published experimental results.[14] This finding will give rise to much interest exploring new possible mechanisms of the anomalous superconducting transition behavior in high pressure phase of silane or exploring other possible superconducting high pressure phases of new metal hydrides.[28–30]

* Electronic address: htwang@nankai.edu.cn/htwang@nju.edu.cn

[1] E. Wigner and H. B. Huntingdon, J. Chem. Phys. **3**, 764 (1935).

[2] N. W. Ashcroft, Phys. Rev. Lett. **21**, 1748 (1968).

[3] C. Narayana, H. Luo, J. Orloff, and A. L. Ruoff, Nature (London) **393**, 46 (1998).

[4] N. W. Ashcroft, Phys. Rev. Lett. **92**, 187002 (2004).

[5] J. Feng, W. Grochala, T. Jaroń, R. Hoffmann, A. Bergara, and N.W. Ashcroft, Phys. Rev. Lett. **96**, 017006 (2006).

[6] C. J. Pickard and R. J. Needs, Phys. Rev. Lett. **97**, 045504 (2006).

[7] J. S. Tse, Y. Yao, and K. Tanaka, Phys. Rev. Lett. **98**, 117004 (2007).

[8] Y. Yao, J. S. Tse, Y. Ma, and K. Tanaka, Europhys. Lett. **78**, 37003 (2007).

[9] G. Gao, A. R. Oganov, A. Bergara, M. Martinez-Canalez, T. Cui, T. Iitaka, Y. Ma, and G. Zou, Phys. Rev. Lett. **101**, 107002 (2008).

[10] X. J. Chen, J. L. Wang, V. V. Struzhkin, H. K. Mao, R. J. Hemley, and H. Q. Lin, Phys. Rev. Lett. **101**, 077002 (2008).

[11] M. Martinez-Canales, A. R. Oganov, Y. Ma, Y. Yan, A. O. Lyakhov, and A. Bergara, Phys. Rev. Lett. **102**, 087005 (2009).

[12] O. Degtyareva, M. Martinez-Canales, A. Bergara, X. J. Chen, Y. Song, V. V. Struzhkin, H. K. Mao, and R. J. Hemley, Phys. Rev. B **76**, 064123 (2007).

[13] X. J. Chen, V. V. Struzhkin, Y. Song, A. F. Goncharov, M. Ahart, Z. X. Liu, H. K. Mao, and R. J. Hemley, Proc. Natl. Acad. Sci. U.S.A. **105**, 20 (2008).

[14] M. I. Eremets, I. A. Trojan, S. A. Medvedev, J. S. Tse, and Y. Yao, Science **319**, 1506 (2008).

[15] O. Degtyareva, J. E. Proctor, C. L. Guillaume, E. Gregoryanz, and M. Hanfland, Solid State Commun. **149**, 1583 (2009).

[16] X. F. Zhou, G. R. Qian, X. Dong, L. X. Zhang, Y. J. Tian, and H. T. Wang, Phys. Rev. B **82**, 134126 (2010).

[17] X. F. Zhou, Q. R. Qian, J. Zhou, B. Xu, Y. J. Tian, and H. T. Wang, Phys. Rev. B **79**, 212102 (2009).

[18] X. F. Zhou, X. Dong, G. R. Qian, L. X. Zhang, Y. J. Tian, and H. T. Wang, Phys. Rev. B **82**, 060102 (R) (2010).

[19] A. R. Oganov and C. W. Glass, J. Chem. Phys. **124**, 244704 (2006).

[20] G. Kresse and J. Furthmüller, Phys. Rev. B 54, 11169 (1996); Comput. Mater. Sci. 6, 15 (1996).

[21] http://www.quantum-espresso.org

[22] J. P. Perdew, J. A. Chevary, S. H. Vosko, K. A. Jackson, M. R. Pederson, D. J. Singh, and C. Fiolhais, Phys. Rev. B **46**, 6671 (1992).

[23] X. F. Zhou, J. Sun, Y. X. Fan, J. Chen, H. T. Wang, X. J. Guo, J. He, and Y. J. Tian, Phys. Rev. B **76**, 100101(R) (2007).

[24] P. B. Allen and R. C. Dynes, Phys. Rev. B **12**, 905 (1975); P. B. Allen, Phys. Rev. Lett. **59**, 1460 (1987).

[25] C. F. Richardson and N.W. Ashcroft, Phys. Rev. Lett. **78**, 118 (1997).

[26] Y. Xie, A. R. Oganov, and Y. M. Ma, Phys. Rev. Lett. **104**, 177005 (2010).

[27] L. L. Sun, A. L. Ruoff, C. S. Zha, and G. Stupian, J. Phys. Condens. Matter **18**, 8573 (2006); **19**, 479001 (2007).

[28] I. Goncharenko, M. I. Eremets, M. Hanfland, J. S. Tse, M. Amboage, Y. Yao, and I. A. Trojan, Phys. Rev. Lett. **100**, 045504 (2008).

[29] T. Scheler, O. Degtyareva, M. Marqués, C. L. Guillaume, J. E. Proctor, S. Evans, and E. Gregoryanz, Phys. Rev. B **83**, 214106 (2011).

[30] D. Y. Kim, R. H. Scheicher, C. J. Pickard, R. J. Needs, and R. Ahuja, arXiv:1104.2313 (unpublished).

Table I. Calculated lattice constants of PtH and Pt_2H at 113, 130, and 160 GPa, compared with that of the $I41/a$ silane at 160 GPa and corresponding experimental results.

Phase	Method	a(Å)	b(Å)	c(Å)	P(GPa)	Reference
PtH	VASP-GGA	2.70	2.70	4.53	113	This work
		2.674	2.674	4.493	130	This work
		2.645	2.645	4.436	160	This work
Pt_2H	VASP-GGA	2.630	2.630	4.471	113	This work
		2.610	2.610	4.437	130	This work
		2.58	2.58	4.38	160	This work
	Experiment	2.671	2.671	4.491	113	14
	Experiment	2.62	2.62	4.39	160	14
SiH_4	VASP-GGA	3.026	3.026	6.818	160	This work
	Experiment	3.035	3.035	6.817	160	14

Table II. Calculated EPC strength λ, logarithmic average phonon frequency ω_{log}, and superconducting transition temperature (T_c) in comparison to other available data under different pressures, for the $P63/mmc$ PtH. The experimental T_c (15 K) corresponds to the measured pressure of 125 GPa.

P (GPa)	113	130	160	192
λ	0.85	0.62	0.53	0.48
ω_{log} (K)	328.66	591.01	658.56	706.74
T_c (K)	17.2 (17[a])	15.1 (15[a])	9.7 (10[a])	7.1 (12[a])

[a]Reference [14].

Figure Captions

FIG. 1. (Color online) Crystal structure of PtH: (a) three-dimensional view, (b) view along the [0001] direction of a $2 \times 2 \times 2$ supercell. The large and small spheres represent Pt and H atoms, respectively, (c) the enthalpy of formation per atom (ΔH) versus the fraction of H (x) in the PtH_x compounds at 113 GPa.

FIG. 2. (Color online) Simulated XRD patterns of the PtH, Pt_2H and $I41/a$ silane structures with the wavelength of 0.3344 Å at 113 GPa (a) and 160 GPa (b) in comparison with the experimental results [14]. The discrepancy for the 111 peak ($2\theta = 10°$) is from the gasket of cubic BN.

FIG. 3. (Color online) Phonon dispersion (a) and electronic band structure (b) of the PtH phase at 113 GPa. The band passes the Fermi level with a flat band in the vicinity of the L point (line with solid squares).

FIG. 4. (Color online) Eliashberg phonon spectral function $\alpha^2F(\omega)$ (solid line) and the EPC strength λ (dotted line) are compared to the phonon density of states (PHDOS) projected on Pt (solid line) and H (dotted line) atoms at 113 GPa.
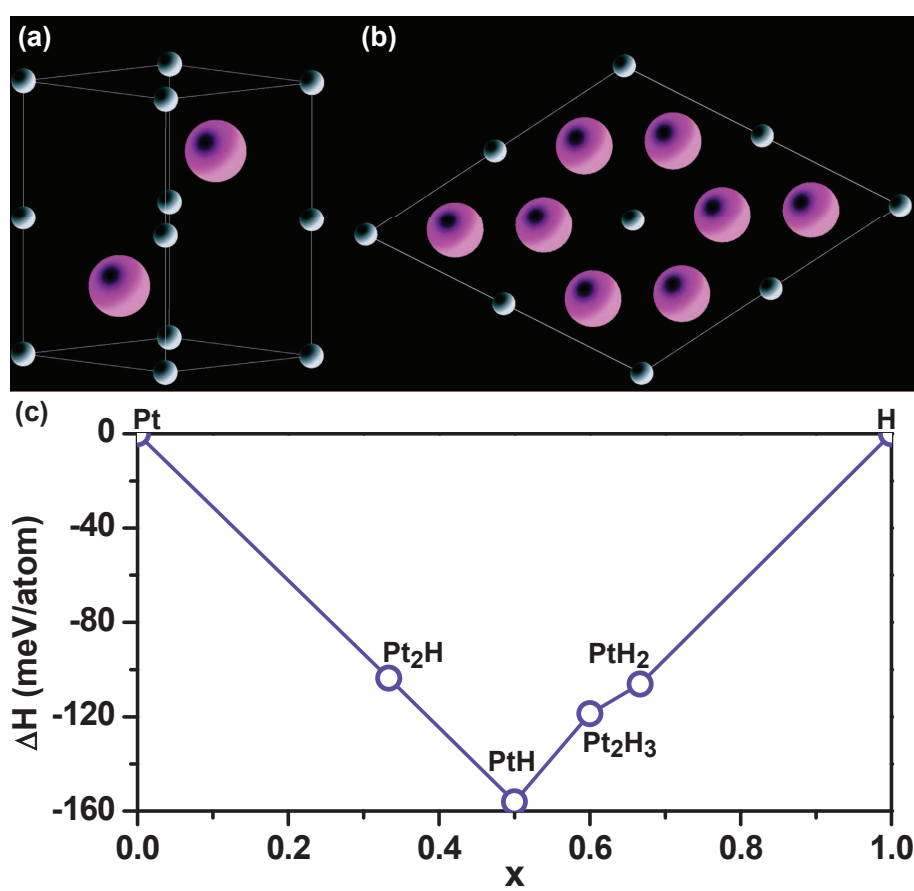
Figure 1   LY12439BR   20Jun2011
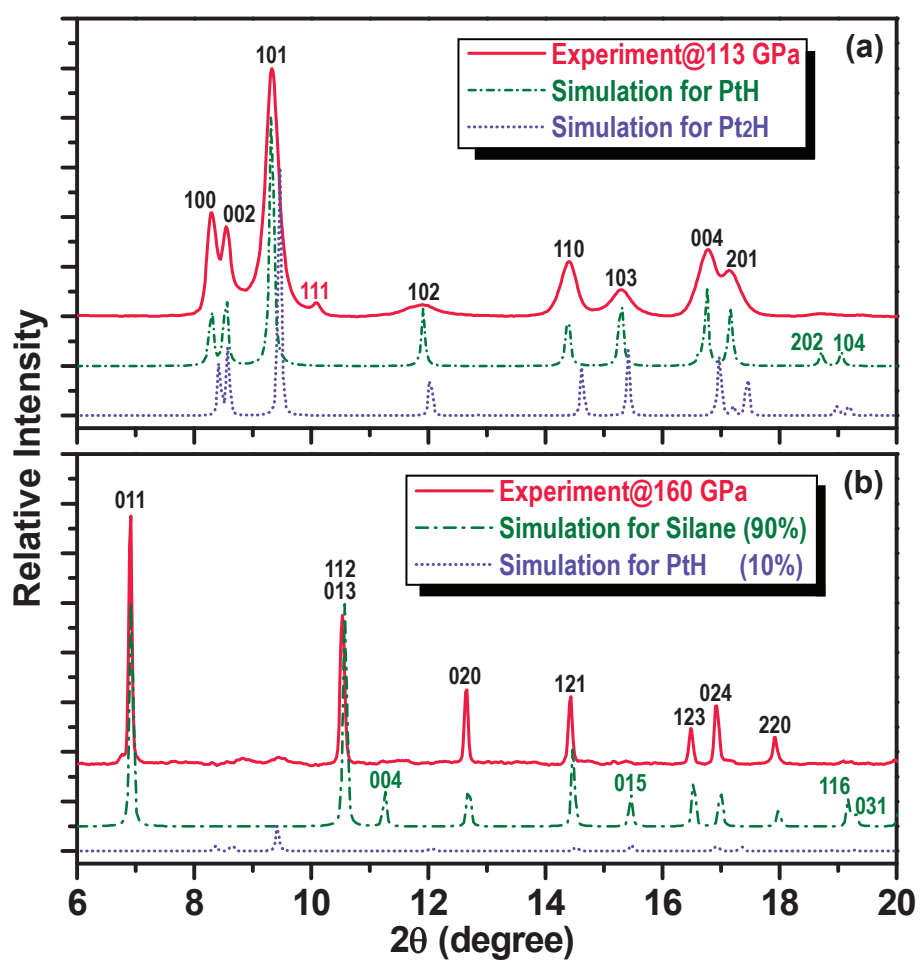
Figure 2   LY12439BR   20Jun2011
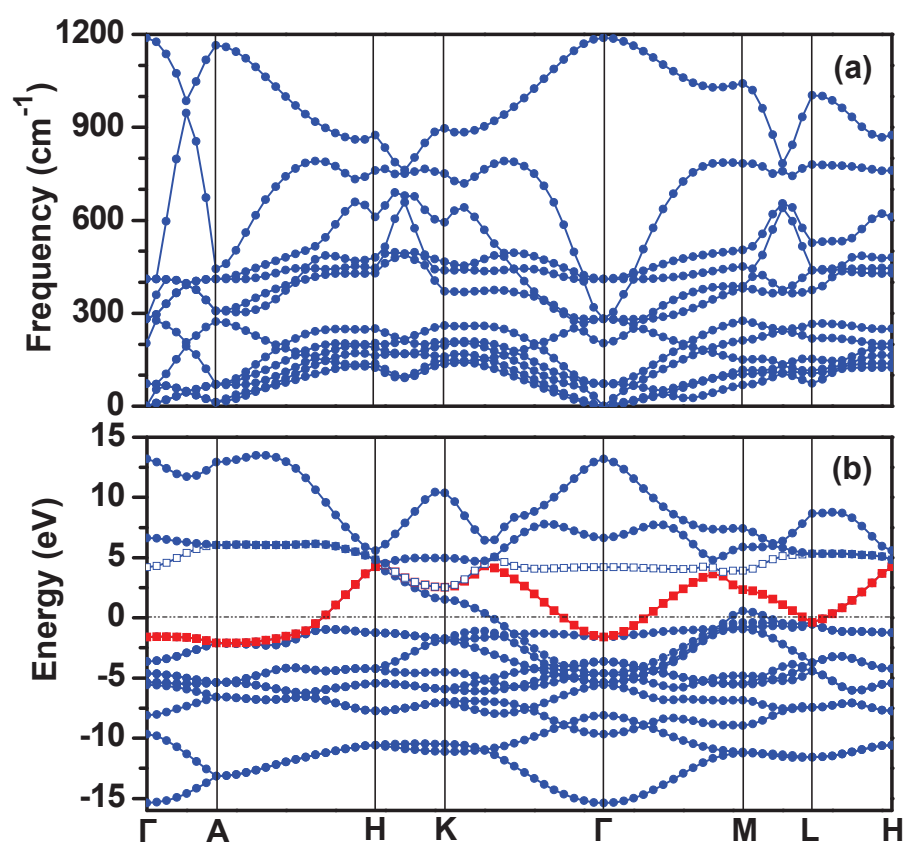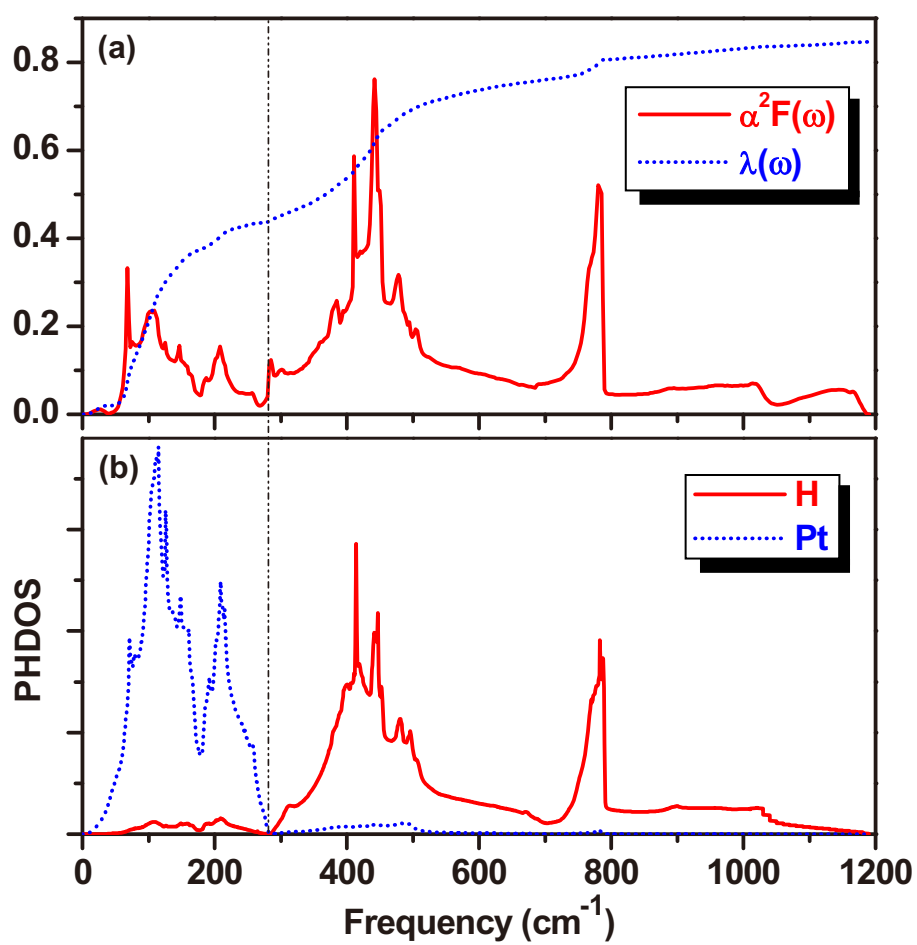
Figure 3   LY12439BR   20Jun2011

Figure 4   LY12439BR   20Jun2011